18TH INTERNATIONAL CONGRESS ON SOUND & VIBRATION
ICSV18
RIO DE JANEIRO
BRAZIL
10–14 JULY 2011

AEROACOUSTIC SOURCE CHARACTERIZATION TECHNIQUE APPLIED TO A CYLINDRICAL HELMHOLTZ RESONATOR

Francisco Rodriguez Verdugo, Roberto Camussi

Department of Mechanical and Industrial Engineering (DIMI), 'Università Roma Tre', 00146 Rome, Italy.
e-mail: frodriguezverdugo@uniroma3.it

Gareth J. Bennett

Department of Mechanical and Manufacturing Engineering, Trinity College, Dublin 2, Ireland.

The aim of this work is to investigate the sound produced by a Helmholtz resonator excited by a boundary layer. A deep cylindrical cavity with a small rectangular opening was designed to allow Helmholtz resonance as well as longitudinal and azimuthal acoustic modes within the cavity to be excited by varying the wind tunnel flow speed. Experiments performed show how lock-on between each of these three acoustic resonances and the shear layer hydrodynamic modes can been generated. The pressure measured by means of a microphone flush mounted with the internal surface of the cavity wall is used to phase-average the planar Particle Image Velocimetry (PIV) data in the shear layer region. The acoustic energy generated is calculated by applying the vortex sound theory developed by Powell and modified by Howe for its application to wall bounded flows. Practically, this can be achieved by extracting the flow velocity and vorticity the from the PIV data and by computing numerically the acoustic particle velocity field. The acoustic sources are localised in space and quantified over an acoustic period providing insight into the sound production of flow-excited cylindrical cavities.

1. Introduction

Numerous engineering applications involve low Mach number flows passing over cavities. These systems are often susceptible to resonance due to feedback between perturbations in the shear layer and the internal pressure of the cavity. This flow-acoustic coupling leads to large unsteady pressure fluctuations and can result in undesirable noise or structural damage. Rockwell and Naudascher[1] have provided an extensive review of shear layer driven cavity flows and have categorised them into three groups: fluid-dynamic, fluid-resonant and fluid-elastic.

Cavities whose openings are partially covered are frequently found in the transportation industry: window buffeting in cars/trains, aircraft landing gear wheel well; in musical instruments: jug bands; and in duct applications: side branches. When these systems are exposed to a grazing flow, two different mechanisms have been identified[3,4]: either periodic compressions of the volume of fluid inside the cavity commonly called Helmholtz resonance or the excitation of a standing acous-

tic wave in the resonator. Both of these mechanisms fall into the Rockwell and Naudascher category of fluid-resonant self-sustaining oscillations and are the mechanisms investigated in this paper. Of particular interest is the measurement and examination of the velocity in the shear layer region when subject to a fluid-resonant condition which has received relatively little attention[6,7,8,9].

Facilitated by the development of full field velocity measurement techniques, acoustic source characterization has interested many researchers[10,11,12,13] in the last decade. The approach is to apply an acoustic analogy to the experimental data in order to identify the spatial distribution of the sound sources. A comparison of the Curle[15] acoustic analogy and the vortex sound theory introduced by Powell[16] and extended by Howe[17], has been recently applied to estimate the cavity sound emission by Koschatzky[14]. According to this study, both analogies correctly estimate the overall sound pressure level; however the vortex sound theory appears to predict better the amplitude of the tonal component.

The present study focuses on a cylindrical Helmholtz resonator excited by a boundary layer. The objective is to characterize the opening regions of the resonator by means of velocity and pressure measurements simultaneously recorded. By applying the vortex sound theory of Howe, the understanding of the spatial distribution of the sound sources is seek.

2. Experimental Setup

A schematic of the current experiment is given in Figure 1. The experiment consists of a 493 mm (*H*) deep cavity with an internal diameter *D* of 238 mm mounted on the lateral wall of a 335 mm long test section with a 125 mm square section (*W*). A draw-down wind tunnel with an elliptical bell-mouth inlet was used to generate a uniform flow in the test section. The diameter of the cavity has been chosen to be as large as possible in order to accommodate azimuthal acoustics modes at frequencies low enough to be excited by a low Mach number flow. Based on preliminary calculations, the two first azimuthal modes are expected to have frequencies of 837 Hz and 1387Hz.

The cavity covering plate was manufactured from a 7.75 mm thick Perplex panel. A rectangular orifice with sharp (45°) chamfered leading and trailing edges was machined into the plate. The opening has a streamwise and a spanwise dimension of L = 45 mm and 40 mm respectively and it is centred in the spanwise direction. The position of the opening is given by Δ, the distance between the trailing edge of the opening and the downstream edge of the cavity (Figure 1). Different covering plates were manufactured, however all the results presented in this paper are for an opening positioned as upstream as possible: Δ = 184 mm.

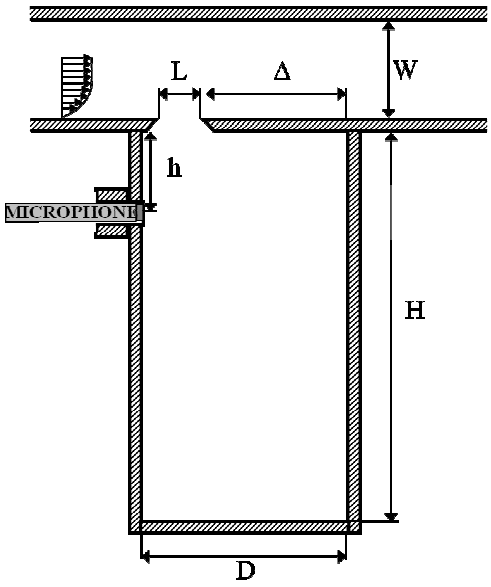

Figure 1. Schematic the experimental rig. Section taken in the central plane. Not to scale.

The wind tunnel flow speed was measured with a Pitot tube located at the end of the test section. The Pitot tube was connected to a pressure transducer Furness Controls FCO 510. A 7 mm diameter G.R.A.S 40PR microphone was used to measure the pressure fluctuations at the upstream lateral of the cavity (h/H = 0.356 in Figure 1). The microphone was connected to an amplifier model PCB Piezotronics 482A16. All the electric signals from the instruments were acquired using a National Instrument PXI-4472B Data Acquisition Card.

The flow in the orifice region was explored with a low speed LaVision PIV system. The seeding particles of DEHS which had a typical particle size of 1 µm were produced by an LaVision aerosol generator. A double pulsed Nd:YAG laser was used to illuminate the flow field. Images were taken with a digital Flow Master CCD camera equipped with a 1279 × 1023 pixel CCD sensor and a 28 mm focal length lens. The images were processed using Davis 7.2 software and the computed velocity fields were exported into Matlab for further post processing. The highest recording rate of the PIV system available was 4 Hz: therefore to resolve the flow field in time, a phase-averaging technique was used.

3. Numerical Simulation of the Acoustic Modes

In order to characterize the acoustic modes of the resonator, a numerical simulation was performed. A highly efficient finite difference method originally introduced by Caruthers[18] was used for the analysis. The approach uses wave functions which are exact solutions of the governing differential equations to interpolate on the grid. The wave expansion method (WEM) code used for this study was developed by Ruiz and Rice[19] and has been examined by Bennett *et al.*[20] for its applicability in ducts.

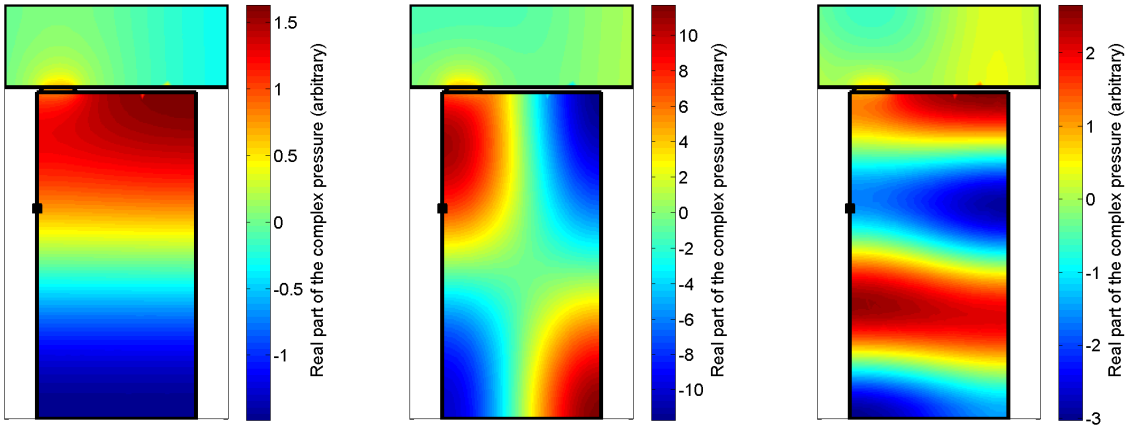

(a) (b) (c)

Figure 2. Numerical solution to a monopole excitation of the cavity and the wind tunnel test section. Three cases: first longitudinal mode H1 (a), first azimuthal-longitudinal mode AZ1H1 (b) and third longitudinal mode H3 (c). Frequencies: 364 Hz, 927 Hz and 1050 Hz. The microphone is indicated by a black square.

A three-dimensional mesh encompassing the wind tunnel test section and the cavity was generated, resulting in approximately 240,000 tetrahedral elements. The code solves the complex pressure in every cell of the mesh. The system was excited by a monopole source located in the geometrical center of the opening. The inlet and the outlet of the test section were modelled with radiation boundary conditions. The response of the system as a function of frequency can be determined by running the code in a loop over many frequencies. Good agreement has been found between the simulation and experiments[9]: in particular, the frequency and the shape of the acoustic modes are correctly predicted. The real part of the complex pressure is plotted in Figure 2 for three different monopole frequencies.

4. Response of the Resonator to a Grazing Flow

The resonator was exposed to a flow of air at room temperature through the wind tunnel. An automated velocity sweep of the tunnel was performed by controlling the centrifugal blower motor speed with LabView. The unsteady pressure inside the cavity was measured with the flush mounted microphone. Results are presented in Figure 3 with the superimposition of the shear layer modes calculated according to Rossiter's[21] formula:

$$St = \frac{fL}{U} \approx \frac{n - \alpha}{M + \frac{1}{\kappa}}. \tag{1}$$

where α describes the phase delay between the hydrodynamic forcing and the acoustic feedback, κ is the convection velocity of the shear layer normalized by the free stream velocity and $n \in \mathbb{N}^*$ is the order of the shear layer mode. For low subsonic speeds as presented here, a number of authors[8,22,23] have argued that there is no need to consider a phase delay when the convection speed is much less than the speed of sound. Therefore $\alpha = 0$ was used. A range of convection speed coefficients are to be found in the literature although often at a value of $\kappa = 0.38$ is used[21]. A value of $\kappa = 0.46$ has been used here as a best fit to the measured data.

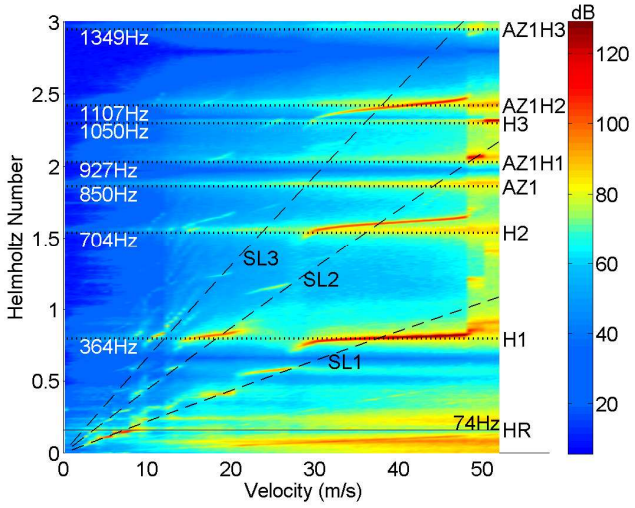

Figure 3. Acoustic response inside the cavity as a function of tunnel flow-speed. Superimposed on the plot are the theoretical shear layer modes (SL), the WEM acoustic modes (H1, AZ1...) and the Helmholtz resonance (HR). Frequencies are given in the non-dimensional form - Helmholtz number: $He = \frac{\pi f D}{c}$.

For a flow speed between 5 m/s and 10 m/s a distinct tone was clearly heard in the testing hall: according to Figure 3, this tone corresponds to Helmholtz resonance excited by the first shear layer instability mode. The resonance frequency measured compares well with the theoretical value of 74 Hz superimposed on Figure 3 and estimated through:

$$f_{HR} = \frac{c}{2\pi}\sqrt{\frac{S}{Vl}}. \tag{2}$$

where c is the sound speed, V the volume of the resonator, S is the plan-view cross section of the orifice (45 mm × 40 mm), l is the equivalent neck length[8] (45 mm).

5. Flow Field

PIV measurements in the orifice region allow greater insight into the fluid dynamics of the shear layer to be obtained. For specific frequencies such as those at lock on, coherent structures were identified and found to be relatively periodic. By using the pressure signal recorded simultaneously with the PIV images, it is possible to compute an average velocity field for a given phase of the acoustic wave. The phase-averaging was possible only when the pressure oscillations dominated the microphone signal: in other words, when the pressure signal can be approximated by a sinusoid. An example of the results is given in Figure 4 where a phase-average velocity and vorticity field are presented. For this study, the 1000 acquired images were divided in 8 different phases. Each phase contains between 100 and 150 PIV realizations.

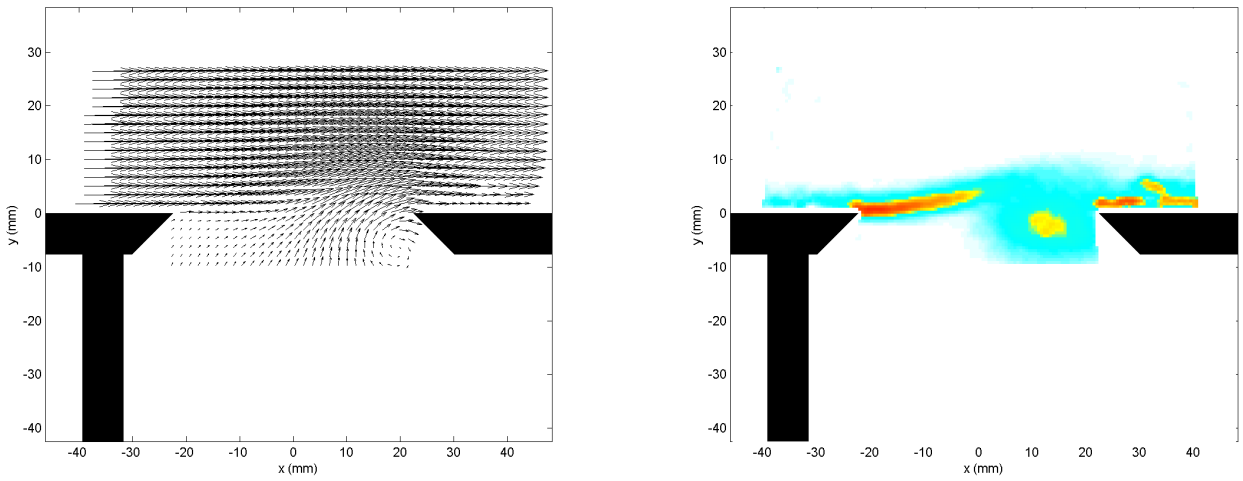

(a) (b)

Figure 4. Phase-averaged velocity (a) and vorticity (b) fields on the orifice region at the phase t / T = 0.25. The free stream velocity of 46 m/s corresponds to a coupling between the first shear layer mode and the first longitudinal acoustic mode (SL1-H1).

6. Acoustic Power

In the Howe[15] vortex sound theory, the Coriolis density forces $\vec{f}_c = -\rho_0\left(\vec{\omega}\times\vec{V}\right)$ are identified as the principal source of sound. The generation of acoustic power by the vortical field can be calculated by the following formula[24]:

$$\Pi = -\rho_0 \int_V \left(\vec{\omega}\times\vec{v}\right)\cdot\vec{u}_{acoust}\,dV\,. \tag{3}$$

where ρ_0 is the mean fluid density, $\vec{v}$ is the velocity, $\vec{\omega}$ is the vorticity and $\vec{u}_{acoust}$ is the acoustic particle velocity. The velocity and the vorticity field can be extracted from the PIV data and the particle velocity numerically from the WEM study. An important assumption in the development followed is that the hydrodynamic quantities (velocity and vorticity) and the acoustic field can be computed independently.

6.1 Computation of the acoustic particle velocity

As seen in Section 3, the numerical simulation gives a complex pressure field whose amplitude depends on the monopole source intensity. In order to dimensionalize the pressure, the experimental data from the flush-mounted microphone was used. It has been assumed that the pressure has a simple harmonic motion in time for any point in the cavity. This assumption is good for

strongly resonant states. Therefore, the pressure P_{acoust} at any point inside the cavity (x,y,z) and at any moment of time (t) can be expressed as:

$$P_{acoust}(x,y,z,t) = cst \cdot P_{WEM}(x,y,z,f_{acoust}) \cdot \sin(2\pi f_{acoust} t). \quad (4)$$

where, P_{WEM} is the pressure from the numerical simulation, f_{acoust} is the frequency of the dominant acoustic mode and *cst* a constant necessary to match the experimental pressure measurements. In order to retrieve the particle velocity field, the linearized Euler momentum equation was used:

$$\rho_0 \frac{\partial \vec{U}_{acoust}}{\partial t} + \nabla P_{acoust} = 0. \quad (5)$$

As an example, the pressure and the acoustic velocity fields in the orifice region are given in Figure 5 for the first acoustic mode.

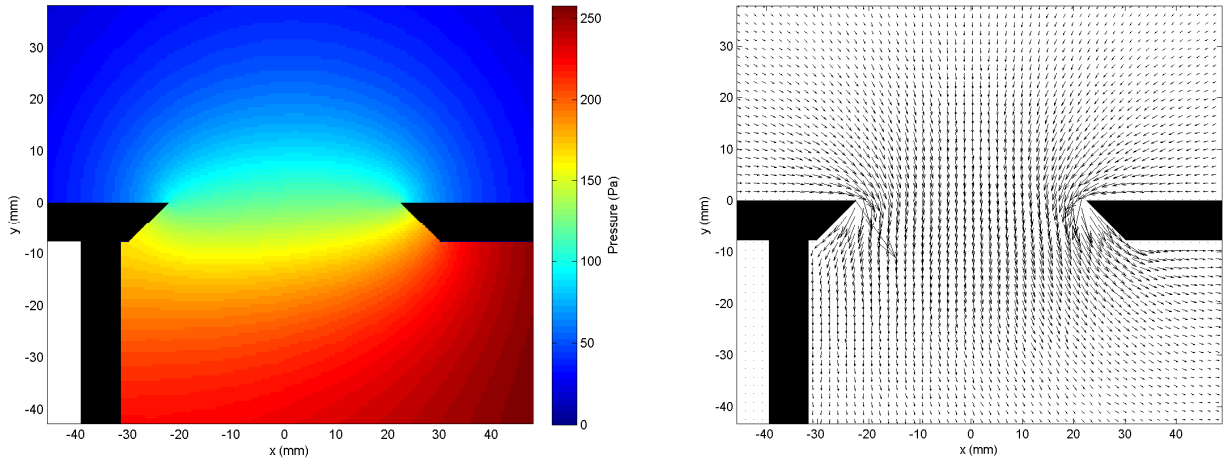

Figure 5. Acoustic pressure field P_{acoust} (a) and acoustic velocity field $\vec{U}_{acoust}$ (b) at the orifice region calculated with the WEM simulation and dimensionalized with the experimental data. First longitudinal mode (H1). Phases (a): $t/T = 0.25$ and (b): $t/T = 0$.

6.2 Time-averaged acoustic power

Three free stream velocities were chosen for the study: 46 m/s, 49 m/s and 51 m/s. These velocities correspond respectively to the first shear layer mode (SL1) locked-on with the first longitudinal mode (H1), the second shear layer mode (SL2) exciting the first azimuthal-longitudinal mode (AZ1H1) and the second shear layer mode (SL2) amplified by the third longitudinal mode H3. The shape of these three acoustic modes is display in Figure 3. The instantaneous acoustic power was found for 8 different phases by computing the integrand of Eq. 3. This intermediary result, even if essential for comprehension of the sound production, is not presented here for sake of brevity.

The acoustic power generated by the vortices in the orifice region over an entire acoustic period can be obtained by averaging the computed instantaneous acoustic powers. The time-averaged acoustic power $\langle \Pi \rangle$ produce by a free stream of 46 m/s (SL1-H1) is given in Figure 6. The pattern calculated is a distinct source-sink pair. This corresponds to the fact that the first shear layer mode is characterized by the generation of a single large-scale vortex over an acoustic period.

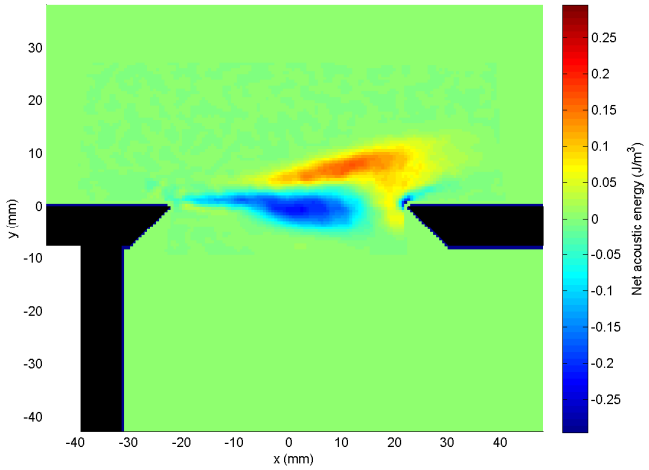

Figure 6. Time-averaged acoustic power. 46m/s, SL1-H1.

The two cases for which the second shear layer mode is dominant are presented in Figure 7. It is interesting to observe the degree of similarity between these two patterns: two source-sink pairs are found above the opening. Again, the shear layer rolling up into large-scale vortices generates this pattern: the second shear layer mode produces two vortices during an acoustic cycle. The major difference between both cases is the sign of the source-sink pairs. It is important to say that the sign of the computed acoustic power depends on the origin of the time axis. The determination of the phase of each PIV realization was done with reference to the pressure measured with the microphone at the upstream wall of the cavity (Figure 1). Therefore the acoustic pressure fluctuations in the orifice region (upstream) are in phase with the fluctuations recorded by the microphone for the AZ1H1 case and out of phase when H3 is dominant (Figure 2 – b, c).

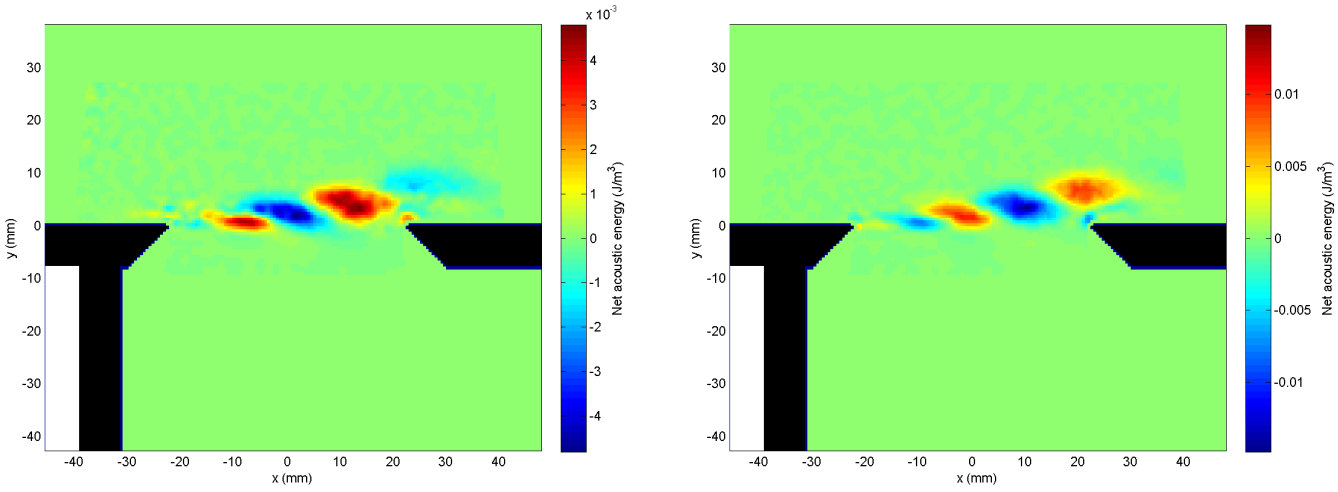

(a) (b)

Figure 7. Time-averaged acoustic power. (a): 49m/s, SL2-AZ1H1. (b): 51m/s, SL2-H3

REFERENCES

1. D. Rockwell and E. Naudascher, "Review - Self-sustaining oscillations of flow past cavities", *Journal of Fluids Engineering* **100**, 152–165 (1978).
2. H. Helmholtz, "Theorie der luftschwingungen in röhren mit offenen enden", *Crelle's Journal* **57**, 1-72 (1860).
3. R.L. Panton and J.M. Miller, "Excitation of a Helmholtz resonator by turbulent boundary layer", *Journal of the Acoustical Society of America* **58**, 800–806 (1975).

4. F.C. De Metz and T.M. Farabee, "Laminar and turbulent shear flow induced cavity resonances", *Proceedings of the AIAA 4th Aeroacoustics Conference*, Atlanta, Georgia, October 3-5 (1977).
5. R.L. Panton, "Effect of orifice geometry on Helmholtz resonator excitation by grazing flow", *AIAA Journal* **28**, 60–65 (1990).
6. S.A. Elder, "Self-excited depth-mode resonance for a wall-mounted cavity in turbulent flow", *Journal of Acoustical Society of America* **64**, 877–890 (1978).
7. P.A. Nelson, N.A. Halliwell and P.E. Doak, "Fluid dynamics of a flow excited resonance, part I: experiment", *Journal of Sound and Vibration* **78**, 15–38 (1981).
8. R. Ma, P.E. Slaboch and S.C. Morris. "Fluid mechanics of the flow-excited Helmholtz resonator", *Journal of Fluid Mechanics* **623**, 1–26 (2009).
9. G.J. Bennett, F.R. Verdugo and D.B. Stephens, "Shear layer dynamics of a cylindrical cavity for different acoustic resonance modes", *Proceedings of the 15th International Symposium on Applications of Laser Techniques to Fluid Mechanics*, Lisbon, Portugal , July 5-8 (2010).
10. M. Geveci, P. Oshkai, D. Rockwell, J.-C. Lin and M. Pollack, "Imaging of the self-excited oscillation of flow past a cavity during generation of a flow tone", *Journal of Fluids and Structures* **18**, 665–694 (2003).
11. C. Haigermoser, "Application of an acoustic analogy to PIV data from rectangular cavity flows", *Experiments in Fluids* **45**, 145–157 (2009).
12. A. Velikorodny, T. Yan and P. Oshkai "Quantitative imaging of acoustically coupled flows over symmetrically located side branches", *Experiments in Fluids* **48**, 245-263 (2010).
13. S. Finnegan, P. Oshkai, and C. Meskell. "Experimental methodology for aeroacoustic source localisation in ducted flows with complex geometry". *Proceedings of the 16th AIAA/CEAS Aeroacoustic Conference*, Stockholm, Sweden, June 7-9 (2010).
14. A. Powell, "Theory of vortex sound", *Journal of Acoustical Society of America* **36**, 177-195 (1964).
15. M.S. Howe, "Contributions to theory of aerodynamic sound, with application to excess jet noise and the theory of the flute", *Journal of Fluid Mechanics* **71**,4, 625–673 (1975).
16. N. Curle, "The influence of solid boundaries upon aerodynamic sound", *Proceedings of the Royal Society of London. Series A, Mathematical and Physical Sciences* **231**,1187, 505-514 (1955).
17. V. Koschatzky, J. Westerweel and B.J. Boersma, "Comparison of two acoustic analogies applied to experimental PIV data for cavity sound emission estimation", *Proceedings of the 16th AIAA/CEAS Aeroacoustic Conference*, Stockholm, Sweden, June 7-9 (2010).
18. J.E. Caruthers, R.C. Engels and G.K. Ravinprakash, "A wave expansion computational method for discrete frequency acoustics within inhomogeneous flows", *Proceedings of the 2nd AIAA/CEAS Aeroacoustics Conference*, State College, Pennsylvania, May (1996).
19. G. Ruiz and H.J. Rice, "An implementation of a wave-based finite difference scheme for a 3-D acoustic problem", *Journal of Sound and Vibration* **256**, 373–381 (2002).
20. G.J. Bennett, C.J. O'Reilly and H. Liu, "Modelling multi-modal sound transmission from point sources in ducts with flow using a wave-based method. *Proceedings of the 16th Congress on Sound and Vibration*, Krakow, Poland, July 5-9 (2009).
21. J.E. Rossiter, "Wind tunnel experiments on the flow over rectangular cavities at subsonic and transonic speeds", *Reports and Memoranda* **3438** (1964).
22. L. Chatellier, J. Laumonier and Y. Gervais, "Theoretical and experimental investigations of low Mach number turbulent cavity flows", *Experiments in Fluids* **36**, 728-740 (2004).
23. M. El Hassan, L. Labraga and L. Keirsbulck, "Aero-acoustic oscillations inside large deep cavities". *Proceedings of the 16th Australasian Fluid Mechanics Conference*, Australia, December 2-7 (2007).
24. M.S. Howe, "The dissipation of sound at an edge", *Journal of Sound and Vibration* **70**, 407–411 (1980).